Research Article

Nano Biomed Eng

Influence of Co Transplantation SnO_2 Nano Film on the Structural and Optical Properties Using Radio Frequency Magnetron Sputtering

Ehssan Hassan[1], Mohamed Odda Dawod[1], Zainab Kadhom Hamzh[2], Marwa Abdul Muhsien Hassan[3]

[1]Department of Physics, College of Science, Mustansiriyah University, Baghdad, Iraq.
[2]College of Science, Mustansiriyah University, Baghdad, Iraq.
[3]Department of Physics, College of Science, Mustansiriyah University, Baghdad, Iraq.

Corresponding author. E-mail: marwamedicalphysics@gmail.com

Received: Apr. 15, 2021; **Accepted:** Dec. 2, 2021; **Published:** Jan. 7, 2022

Citation: Ehssan Hassan, Mohamed Odda Dawod, Zainab Kadhom Hamzh, and Marwa Abdul Muhsien Hassan,Influence of Co Transplantation SnO_2 Nano Film on the Structural and Optical Properties Using Radio Frequency Magnetron Sputtering. *Nano Biomed. Eng.*, 2022, 14(1): 1-6.
DOI: 10.5101/nbe.v14i1.p1-6.

Abstract

In this research, investigated characterization of pure and Cobalt doped Tin dioxide SnO_2:Co with 3, 5 and 7wt% fabricated using radio frequency magnetron sputtering method deposited on glass surfaces. The results showed that prepared SnO_2:Co were nano films and poly crystalline in form with favored reflection permanently (110) plan, and the crystallite size decreases as the Co concentration increased 9-14 nm. The optical properties represented by the transmittance of perspicuous and cobalt transplantation SnO_2 layers were studied and results showed that highest transmittance obtained was 91% in the pure films and decreased to 78% as the Co concentration increased; the wavelength range was 300-900 nm due to be the increasing of the Co amount during the deposition, leading to a linear increase in mobility and carrier concentration, until a threshold of Co content was overcome and from that point onward the mobility began to decrease. Optical energy gaps of perspicuous and Co transplantation SnO_2 nano layers were determined and the energy gap was reduced from 3.50 eV of perspicuous nano layers to 3.29 eV for the highest transplantation concentration.

Keywords: RF sputters, Co doped SnO_2, Radio frequency of 13.56 MHz, EDXS measurement

Introduction

Tin oxide (SnO_2) a tetragonal rutile assembly with grid parameters a = b = 4.737 Å and c = 3.826 Å [1]. The structure of unit cell includes two tins and four oxygen atoms. Each tin atom is attached or bound to six oxygen particles at the edges of a customary octahedron, and each oxygen atom is encompassed by three tin particles [2]. Tin dioxide SnO_2-based thin layers have been generally contemplated in light of the fact that they are steady towards environmental conditions, artificially inactive and precisely hard and they can oppose high temperatures [3]. Notwithstanding their applications as optical windows for the sun-based range [4], delicate switches [5], computerized shows [6], electro chromic shows [7] and gas sensors [8]. Unadulterated and doped-SnO_2 thin film of different dopants have been set up by diverse procedures, for example, magnetron sputtering [9], sol-gel strategy [10], chemical vapor deposition (CVD) [11] and pulsed laser deposition [12]. Among these procedures, RF magnetron sputtering technique has a basic and cheap

exploratory plan and has the points of interest like the simplicity of including dopants, blade development rate and uniform enormous territory coatings. Doping of different metals with transmission conduction oxide layers has been exhibited to be a straight forward and powerful approach to improve the movie qualities and henceforth endeavors have been made toward this path targeting expanding the conductivity, transmission and solidness of different TCOs. Doping is additionally regularly used to change the conductivity and detecting properties of oxide films [13]. The SnO_2 films are n-type semiconductors with a direct optical band hole of about (3.6-4.3) eV [14]. The SnO_2 is picked on account of its high electrical conductivity and its straight forwardness in the noticeable and infrared light [14-16].

Experimental

Sputtered target was a mixture of high pureness tin dioxide powder and Co (3%, 5% and 7%) wt% high purity 99.998% made in Germany. To shape a target with 50.0 mm in diameter and 3.50 mm width, the blended powder was pressed lower of 4.0 ton press. Target obtained was as thick and homogeneous as possible in order to ensure better deposit performance. Layer was deposited on a glass substrate Superior w. Germany, using Radio Frequency magnetron sputter setup TORR INTERNATIONAL, INC. CRC600. The sputtering space was emptied to an illustrated pressure of 7.4×10^{-6} Torr by the combination of oil pump, rotary and turbo molecular pump before the ignition of the plasma, the deposition power was fixed at 150 W (rs-130) at a frequency of 13.56 MHz. The angel was 45° through electrodes and surface point, the distance through target and glass surface was 10 cm. Drift rate of Argon gas was immobile to 30 sccm by the Ailcat mass flow controller. The SnO_2:Co films were deposited at an employed compressing of 0.0001 Torr and radio hesitation energy of 13.6 megahertz.

Result and Discussion

Structure and morphology

Fig. 1 observed that the major reflection on the pure and Co doped SnO_2 nano films is (110) plan at the angle $2\theta = 26.61°$, which was approved in calculating the crystallite size, microstrain and dislocation density, which were also inferred to the standard JCPDS card No. 41-1445 [17]. The XRD pattern of deformed nano layers, observe that acuteness for the preferred reflection (110) plan for all deposited nano layers decreases the crystallization intensity and the crystallite size as the condensation of doping increases, Because of this difference in ionic size between the Co^{+2} 0.07 nm and the Sn^{+2} 0.118 nm where the cobalt ions tend to fill. The sites of the vacnces in the lattice, which produces stress on the tin ions, leading to a decrease in the crystallization of the preferred reflection (110). Mainer reflections (101), (200) and (211) appear

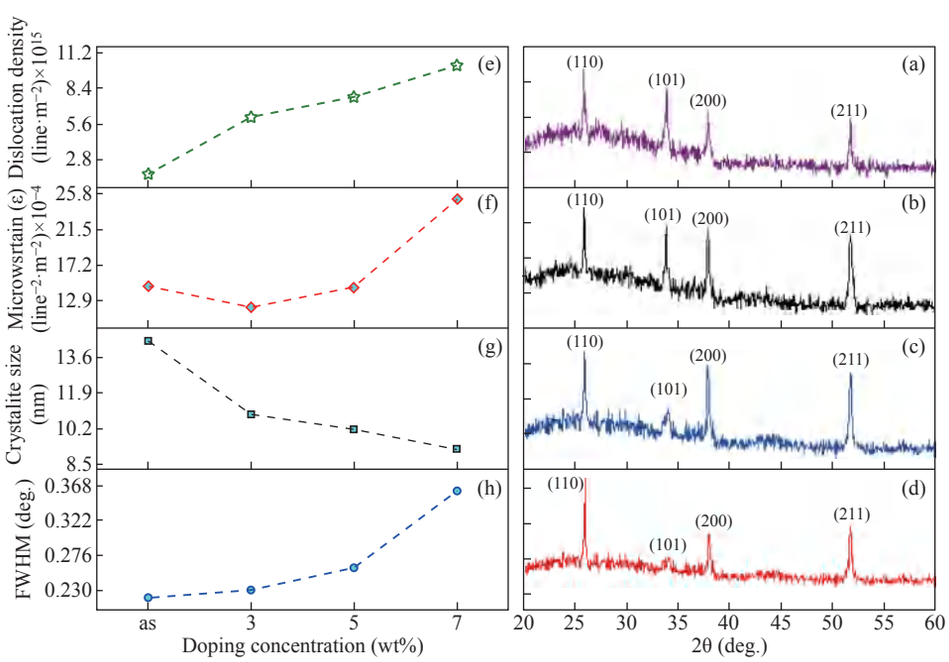

Fig. 1 X-Ray diffraction **(a)** as deposited SnO_2, (**(b)**, **(c)** and **(d)**) 3wt%, 5wt% and 7wt%, respectively Co doping concentration, **(e)** Dislocation density, **(f)** Microstrain, **(g)** Crystallite size and **(h)** FWHM.

Table 1 Structural properties of SnO_2:Co nanofilms fabricated by radio frequency magnetron sputtering

Doping concentration (wt%)	hkl	FWHM (Degree)	2θ (Degree)	Crystalite size (nm)	Microstrain (line^{-2}/m)×10^{-4}	Dislocationdensity (δ) (line/m²)×10^{15}
as	(110)	0.36	26.43	9.22	25.08	1.176
	(101)	0.34	34.31	12.35	30.12	1.304
	(200)	0.33	38.98	11.63	26.64	1.261
	(211)	0.35	50.52	13.72	21.08	1.432
3%	(110)	0.22	26.91	10.13	14.37	9.746
	(101)	0.23	34.49	9.88	15.72	10.162
	(200)	0.21	38.12	13.24	16.47	12.036
	(211)	0.24	50.31	10.98	14.88	8.332
5%	(110)	0.23	26.98	10.87	12.07	8.459
	(101)	0.22	34.87	11.56	10.46	8.672
	(200)	0.24	38.76	14.08	13.77	10.144
	(211)	0.21	50.65	12.53	16.05	9.463
7%	(110)	0.26	26.54	14.39	14.62	4.830
	(101)	0.25	34.43	13.57	15.92	5.962
	(200)	0.23	38.32	13.11	16.44	6.021
	(211)	0.24	50.21	11.99	14.52	5.883

at 2θ = 34.26°, 38.01° and 51.75 respectively as in Fig. 1(a)-(d) the variation in the reflection intensity is due to increase in the dopant concentration. The crystallite volume was estimated by Debye Scherrer's relation (1) and result shows that the increasing of doping condensation decreased the crystallite volume as observed in Fig. 1(g). This is attributed to the replacement of relatively bigger Sn^+ ions by the relatively smaller Co^+ ions during the formation of the SnO_2:Co nano films. As the radius of Co ion is smaller than that of tin ion. Fig. 1(f) observed the Micro-strain in the layers which has been valued from the equation 2, increases with accretion of Co concentration, which may reason by decreasing in the crystallinitity of the layer [18]. Dislocation density (δ) has been estimated using relation number (3) and Fig. 1(e) observed that dislocation density increases with accretion of the Co concentration [19]. Table 1 includes outcomes values of microstrain, crystallite size and dislocation density.

$$D = (k\lambda)/(\beta\cos\theta), \quad (1)$$

$$\delta\varepsilon = 1/D^2, \quad (2)$$

and

$$\varepsilon = (\beta\cos\theta)/4, \quad (3)$$

where D is crystallite size, k is constant number, λ is wavelength, δ is dislocation density, ε is microstrain, and β is full width at half maximum.

SnO thin films can exhibit either tetragonal or orthorhombic structure. Kim and co-authors reported SnO thin films with tetragonal structure after annealing at a temperature of 300 °C by using RFsputtering with a SnO/Sn (9:1 mol% ratio) composite target.

Fig. 2 shows an SEM image and EDXS measurements for Co doped SnO_2 nanostructure deposited using radio frequency magnetron sputtering. Fig. 2(a) seen that nano film consisted of nano particle matters and varying from 40 nm to 70 nm, and as the Co concentration increasing form 3wt% to 5wt% that showed in Fig. 2(b) the particle size decreased and ranged between 23 nm to 50 nm. Further increases in the Co concentration up to 7 wt% as in Fig. 2(c) the particle size range around 30 nm to 40 nm. All deposited samples show very smooth and homogeneous surface and no further contamination found at the EDS measurement displays.

The transmittance of the pure SnO_2 and SnO_2: Co thin films deposited on glass substrate using radio frequency magnetron sputtering technique is calculated by using equation (4) [20].

$$T = \exp[-2.303A] \quad (4)$$

From Fig. 4, the transmittance spectrum of all deposited thin films increases with the increasing of wavelength (λ) (200–900) nm. On the other hand, the

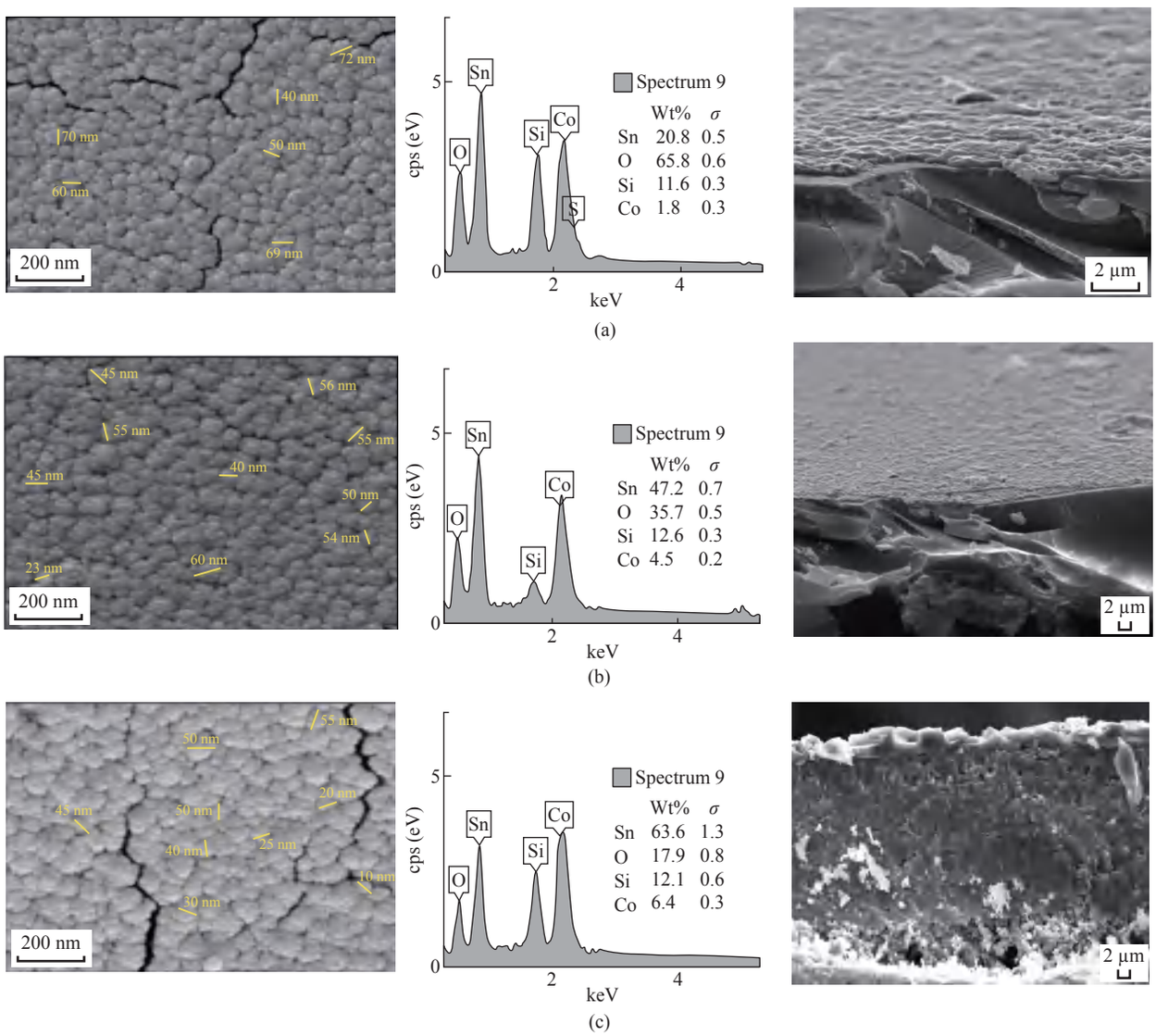

Fig. 2 SEM and EDXS of SnO_2:Co **(a)** 3wt%, **(b)** 5wt% and **(c)** 7wt%.

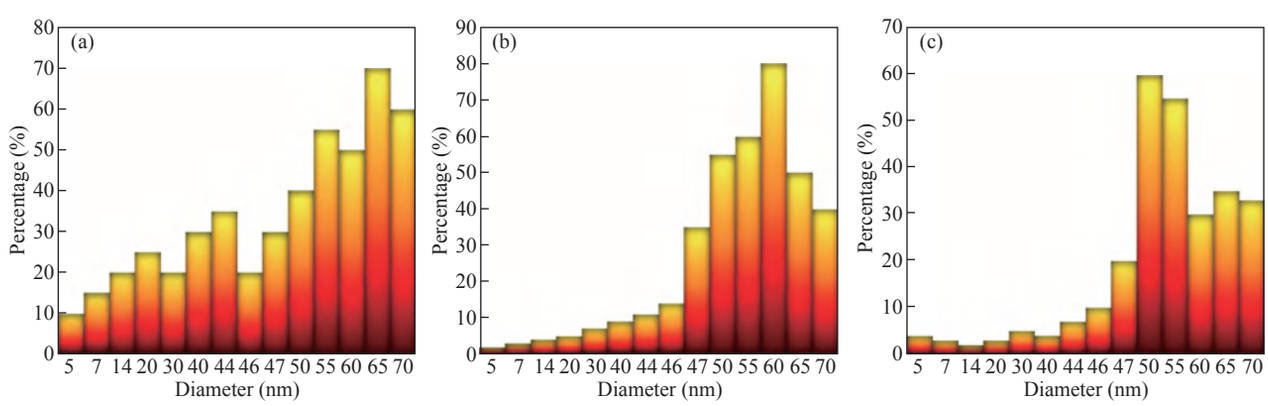

Fig. 3 Relation between diameter and percentage for SnO_2:Co **(a)** 3wt%, **(b)** 5wt% and **(c)** 7wt%.

transmittance spectrum increases with the adding of Co and this is due to the decrease of the surface roughness promoting the decrease of the surface scattering of the light. The transmittance of pure and SnO_2:Co films were shown in Fig. 4, the transmittance was found to increase sharply in the wavelength of 450 nm, and then gradually increases with wavelength. The maximum transmittance observed for un-doped SnO_2 was almost (91%), while for the doped films was around 86% to 78%. The optical transmission values are

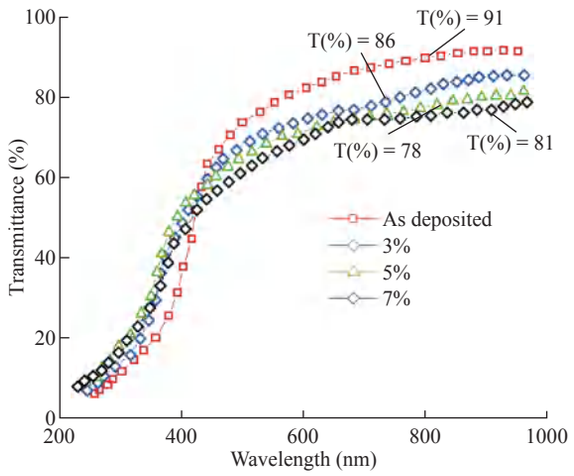

Fig. 4 Transmittance (%) versus wavelength for SnO_2 and Co doped SnO_2 films.

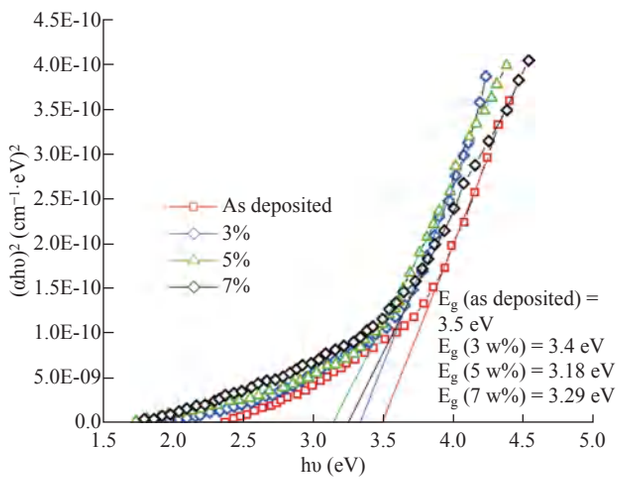

Fig. 5 $(\alpha h\upsilon)^2$ versus photon energy for perspicuous and Cobalt transplantation SnO_2.

decreasing with the increase cobalt concentration this behavior is may be due to the decreases in crystallite volume as measured using X-Ray diffraction and SEM observation the lower transmittance indicates higher defect density of the SnO_2:Co films caused by crystalline defects such as grain boundaries and dislocations [20].

The optical energy gap

The direct energy gap was estimated for the relation (4), the direct band gap has been found to decline by increasing the doping percentage (3wt% and 5wt %) and increasing the band gap when doping increase at 7wt% due to the shift from Moss-Burstein [21-25].

Conclusions

In this paper, a methodology to obtain both pure and dopped SnO_2:Co thin films with tetragonal structure and similar chemical stoichiometry by RF magnetron sputtering using a target of pure tin is proposed. The maximum transmittance observed for un-doped SnO_2 was almost (91%), while for the doped films was around 86% to 78%. The optical transmission values are decreasing with the increase cobalt concentration this behavior is may be due to the decreases in crystallite volume as measured using X-Ray diffraction and SEM observation the lower transmittance indicates higher defect density of the SnO_2:Co films caused by crystalline defects such as grain boundaries and dislocations. This has resulted in decreasing the crystalline volume as demonstrated by structural measurements and SEM pictures, as well as the reduction of energy gap values due to the weakening of crystallization but not continuously the values of 7% increased the values of the energy gap by the effect of increasing the free shipping carriers in the energy gap.

Conflict of Interests

The authors declare that no competing interest exists.

Authors' Contribution

Ehssan Hassan contributed to 40% of the work, Mohamed Odda Dawod 30%, and Marwa Abdul Muhsien Hassan 30%.

Acknowledgments

This research was propped by University of Mustansiriyah, College of Science, Department of Physics, Tribology and advanced materials Lab. and the group labor would like to thank the Ministry of Science and technology for provided that the needful backing and advice for RF-magnetron sputtering setup. Financial grants in this paper were not achieved from any foundation.

References

[1] V. Gokulakrishnan, S. Parthiban, K. Jeganathan, et al., Investigations of the Structural, Optical and Electrical Properties of Nb-Doped SnO_2 Thin Films. *J. Mater Sci.*, 2011, 4: 65553-5558.

[2] A. Rydosz, A. Brudnik, and K. Staszek., Metal Oxide Thin Films Prepared by Magnetron Sputtering Technology for Volatile Organic Compound Detection in the Microwave Frequency Range. *Materials (Basel)*, 2019, 12(6): 877.

[3] Y. Ma, X. Zhang, W. Liu, et al., Stoichiometry Dependence of Physical and Electrochemical Properties of the SnOx Film Anodes Deposited by Pulse DC Magnetron Sputtering. *Materials*, 2021, 14(7): 1803.
[4] L. Wang, L. Yin, Metal Oxide Gas Sensors: Sensitivity and Influencing Factors. *Sensors*, 2010, 10: 2088-2106.
[5] Z. Florian, B. Daniel, Tin oxide-based nanomaterials and their application as anodes in lithium-ion batteries and beyond. *Chem Sus Chem*, 2019, 12: 4240-4259.
[6] C. Kim, S. Kim, and S.E. Kim, Transparent SnOx thin films fabricated by radio frequency reactive sputtering with a SnO/Sn composite target. *Thin Solid Films*, 2017, 634: 175-180.
[7] Thin Solid Films. 2017; 634: 175-180.
[8] E. Eqbal, R. Raphael, K.J. Saji, et al., Fabrication of p-SnO/n-SnO_2 transparent p-n junction diode by spray pyrolysis and extraction of device's intrinsic parameters. *Mater Lett*., 2019, 247: 211-214.
[9] V. Gokulakrishnan, S. Parthiban, Investigations on The Structural, Optical and Electrical Properties of Nb-Doped SnO_2 Thin Films*, J. Mater Sci.*, 2011, 46: 5553-5558.
[10] S.D. Nehate, A. Prakash, Work function extraction of indium tin oxide films from MOSFET devices. *ECS J Solid State Sci Technol*., 2018, 7(3): 87-90.
[11] D.E. Guzmán-Caballero, M.A. Quevedo-López, and R. Ramírez-Bon, Optical properties of p-type SnO_x thin films deposited by DC reactive sputtering. *J Mater Sci Mater Electron*, 2019, 30(2): 1366-1373.
[12] S. Vallejos, F. Di Maggio, T. Shujah, et al., Chemical Vapour Deposition of Gas Sensitive Metal Oxides. *Chemosensors*, 2016, 4(4).
[13] J. Adawiya, S. Haider, S. Shaker, et al., A study of morphological, optical and gas sensing propertiesfor pure and Ag doped SnO_2 prepared by pulsed laser deposition (PLD). *Energy Procedia*, 2013, 36: 776-787.
[14] C. Sankara, V. Ponnuswamy, M. Manickama, et al., Structural, morphological, optical and gas sensing properties of pure and Ru doped SnO_2 thin films by nebulizer spray pyrolysis technique, 2015, 349(15): 931-939.
[15] T. Le, H.P. Dang, and V.H. Le, Determination of the optimum annealing temperature and time for Indium-doped SnO_2 films to achieve the best p-type conductive property. *Journal of Alloys and Compounds*, 2017, 696 (5): 1314-1322.
[16] N.H. Hong, J. Sakai, W. Prellier, et al., Transparent Cr-doped SnO_2 thin films: ferromagnetism beyond room temperature with a giant magnetic moment. *Phys.: Condens. Matter*, 2005, 17(10): 1697.
[17] S. Zhuang, X. Xu, Y. Pang, et al., Variation of structural, optical and magnetic properties with Co-doping in $Sn_{1-x}Co_xO_2$ nanoparticles. *Journal of Magnetism and Magnetic Materials*, 2012, 40(9).
[18] Joint Committee on Powder Diffraction Standards (JCPDS). *International Centre for Diffraction Data*, 1997, Card No. 41-1445.
[19] N.F. Habubi, G.H. Mohamed, and S.F. Oboudi, Structural and electrical properties of cobalt doped SnO_2 thin films. *MSAIJ*, 2014, 11(10): 321-326.
[20] S.Y. Wang, B.L. Cheng, C. Wang, et al., Dielectric properties of Co-doped $Ba_{0.5}Sr_{0.5}TiO_3$ thin films fabricated by pulsed laser deposition. *Journal of Crystal Growth*, 2003, 259 (1): 137-143.
[21] B.P. Uberuaga, L.J. Vernon, and E. Martinez, The relationship between grain boundary structure, defect mobility, and grain boundary sink efficiency. *Sci Rep*., 2015, 5: 90-95.
[22] J.W. Morris Jr., Chapter 4: Defects in Crystals, *Materials Science*, 2016.
[23] M.A.M. Hassan, A.A. Hateef, Amperometric biosensor of SnO_2 thin film modified by Pd, In and Ag nanostructure synthesized by CSP method. *Applied Nanoscience*, 2014, 4: 927-934.
[24] M.A. Muhsien, E.T. Salem, Gas sensing of Au/n-SnO_2/p-PSi/c-Si heterojunction devices prepared by rapid thermal oxidation. Applied Nanoscience, 2014, 4: 719-732.
[25] M.A. Muhsien, Y. Al-Douri, E.T. Salim, et al., Synthesis of SnO_2 nanostructures employing Nd:YAG laser. Applied Physics A, 2015, 120(2).
[26] M.A. Muhsien, E.T. Salem, and I.R. Agool, Preparation and Characterization of (Au/n-Sn/Si/Si/Al) MIS Device for Optoelectronic Application. *International Journal of Optics*, 2013, 9.